Journal of Hydroscience and Hydraulic Engineering
Vol. 8, No. 2, December, 1990, 39-52

EFFECTS OF CHANNEL SHAPE AND FLOODPLAIN ROUGHNESS ON FLOW STRUCTURE IN COMPOUND CROSS SECTION

By

Akira Murota

Professor, Osaka Sangyo University, Daito, Osaka, Japan

Teruyuki Fukuhara

Associate Professor, Fukui University, Bunkyo, Fukui, Japan

and

Masanori Seta

Ministry of Construction, Chiyoda, Tokyo, Japan

SYNOPSIS

A series of experiments were carried out to measure the mean velocity, turbulence intensity and boundary shear stress distributions in compound channels with rough floodplains. Three different floodplain widths, main channel widths and heights were combined to understand the effects of varying channel geometry, size, the ratio of flow depth to main channel depth and roughness elements on the floodplains. From the present study, a strong relation was observed between the mean velocity structure, turbulence structure and shear distribution. It was found, especially, that the roughness elements on the floodplains strongly affects the flow structures in the compound channel.

INTRODUCTION

The structures of the mean velocity, turbulence intensity and wall shear stress are deeply related to the conveyance of flows in compound channels. Since discharge assessment is one of the main purposes of the research on compound channel flows, it is important to obtain many data on macroscopic flow structures and find the influence of channel geometry and floodplain roughness on flows in compound channels. Rajaratnum et al.(17) discussed the similarity of the mean velocity-profile with varying of the ratio of water depth in the main channel to the height of the main channel, H/D. Imamoto and Kuge(9) showed the variations of the mean velocity, turbulence intensity and Reyolds stress distributions in the cross section when H/D and the width of floodplain, B_f, were changed. Prions et al.(15) measured the turbulence intensity and Reynolds stress profiles and discussed the effects of the floodplain roughness on the turbulence structure. Yen and Overton(19) also presented the iso-velocity contours in compound channel flows with rough and smooth boundary. Gosh and Jena(6) investigated the variation of the distributions of wall shear stress due to the interaction between the main channel and floodplain flow. Knight and Demetriou(12) measured the average shear forces acting on different boundaries of a compound section and discussed the general features of the apparent shear force. Wormleaton et al.(20) obtained the apparent shear stress acting on the vertical interface between the floodplain and the main channel and examined its characteristics.

Though it has been recognized that the exchange flow between the main channel and the floodplain must play an important role in the flow resistance, its characteristics have not yet been well applied to the discharge assessment , because of the lack of information about the interaction between the main channel

and floodplain flow. Imamoto and Ishigaki(7) discussed the relationship between the secondary flows and boiling currents towards the water surface near the main channel/floodplain junction. Fukuoka and Fujita(5) investigated the effects of H/D, channel shape and size and floodplain roughness on the three dimensional large-scale eddies, which can be observed at the main channel/floodplain junction. Tominaga et al. (18) evaluated quantitatively the contribution of secondary flows to spanwise momentum transport from the main channel to the floodplain. Flow structures in a compound channel with floodplain roughness, however, still have many unknown aspects, and the number of related papers is also still minimal .

Recently, Radojkovic et al.(16), Bommanna et al.(3), Alavian et al.(1), Pasche et al.(14) and Kawahara and Tamai(10) presented the numerical results of the relationship between the water level and discharge, and reproduced the flow structure by using mathematical models. The present study may offer significant information about the validity of mathematical models such as the k-ε model.

This paper is aimed at studying the influence of channel geometry and floodplain roughness on the velocity, turbulence intensity and wall shear stress profiles in compound channel flows. To this purpose, the floodplain width, main channel width and height of the main channel were changed systematically, and roughness elements were set on the floodplains.

EXPERIMENTAL METHOD AND CONDITIONS

Experiments were conducted in a rectangular channel 20m long, 0.7m wide and 0.3m deep with a smooth wall, which was made of acrylic resin. The compound cross section, as in Fig.1, was composed of acrylic resin 10m in length. Acrylic resin strips with 5mm square were used as roughness elements, and were placed on the floodplains, at intervals of 20mm, in the transversewise direction. In this case, an imaginary bed rises 4mm from the actual bed because of a separation of flow due to the large number of roughness elements. The main channel was hydraulically smooth and its Manning's roughness coefficient, n_m, was 0.01.

Experimental conditions are presented in Table 1. The compound sections were set up by three different variables : the depth of the main channel, D, the width of the main channel, B_m, and the width of the floodplain, B_f. In order to recognize the hydraulic effect of the floodplain roughness on the flow structures, two kinds of compound cross sections were used under the same geometry and size, that is, the same B_m, B_f and D. One of the two is called Type-S and Manning's n of the floodplains, n_f and n_m are same each other. The other is called Type-R, which has a smooth main channel and floodplains with roughness elements, i.e. $n_f > n_m$. In Table 1, Q_{max} and Q_{min} denote the maximum discharge and minimum discharge. H_{max} and H_{min} correspond to the flow depth in the main channel for Q_{max} and Q_{min}, respectively. The value of n_f expresses Manning's n for Type-R when H/D is 2.0.

Streamwise velocity, U was measured simultaneously with a φ3mm propeller current meter and a hot-film anemometer . The latter was especially convenient to measure U near the walls. The wall shear stress, τ_w was calculated by the

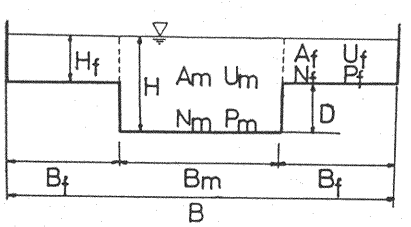

Fig. 1 Illustration of compound channel section

Table. 1 Experimental conditions

CASE	B_f (m)	B_m (m)	D (m)	H_{max} (m)	H_{min} (m)	Q_{max} (cc/s)	Q_{min} (cc/s)	n_f ($m^{-1/3}s$)	n_m
R-15-40-3	0.146	0.4	0.029	0.0745	0.0348	10700	2930	0.023	0.01
R-20-30-3	0.196	0.3	0.029	0.0898	0.0341	9230	1850	0.023	0.01
R-25-20-3	0.246	0.2	0.029	0.0718	0.0380	5600	1550	0.023	0.01
R-15-40-5	0.146	0.4	0.049	0.0995	0.0588	15700	5990	0.023	0.01
R-20-30-5	0.196	0.3	0.049	0.0989	0.0584	12500	4180	0.023	0.01
R-25-20-5	0.246	0.2	0.049	0.0923	0.0590	7170	2510	0.023	0.01
R-15-40-7	0.146	0.4	0.070	0.1316	0.0839	21190	9440	0.023	0.01
R-20-30-7	0.196	0.3	0.070	0.1283	0.0840	12070	4060	0.023	0.01
R-25-20-7	0.246	0.2	0.070	0.1278	0.0847	16220	7170	0.023	0.01
S-15-40-5	0.150	0.4	0.047	0.0937	0.0572	18000	6900	0.010	0.01
S-20-30-5	0.200	0.3	0.047	0.0947	0.0571	15550	4880	0.010	0.01
S-25-20-5	0.250	0.2	0.047	0.0937	0.0568	12030	3280	0.010	0.01

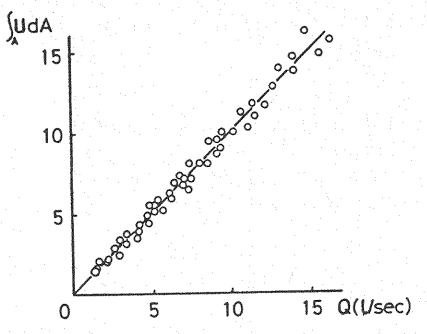

Fig. 2 Accuracy of velocity measurement

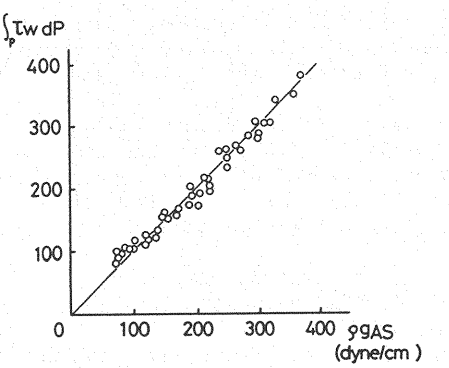

Fig. 3 Accuracy of wall shear stress

logarithmic law of velocity profile. An accuracy of U was confirmed by the continuity equation, $Q=\int_A UdA$, where A is the total flow sectional area of the compound channel. An accuracy of τ_w can be checked by making a comparison of the total boundary shear force with the component of weight in the direction of flow. It is apparent from Figs.2 and 3 that errors in measurement of U and τ_w were less than $\pm$ 5% in all experimental cases.

RESULTS AND DISCUSSIONS OF MEAN VELOCITY

Characteristics of Iso-velocity Contours

Figure 4 shows the iso-velocity contours in the cross section of compound channel and the characteristics of their profiles are explained in terms of the following hydraulic parameters, i.e. the relative water depth, H/D, floodplain roughness, B_f, $B_m(=1-2B_f/B)$ and D.

(A) Effects of relative water depth

(1) When H/D is large, the maximum velocity in the floodplains occurs below the water surface, regardless of Type-R or Type-S.

(2) In the case of Type-S, a high velocity region appears on the floodplain near the floodplain/main channel junction. Imamoto et al.(8) and Fukuoka et al.(4) already have pointed out the existence of the high velocity region. This means

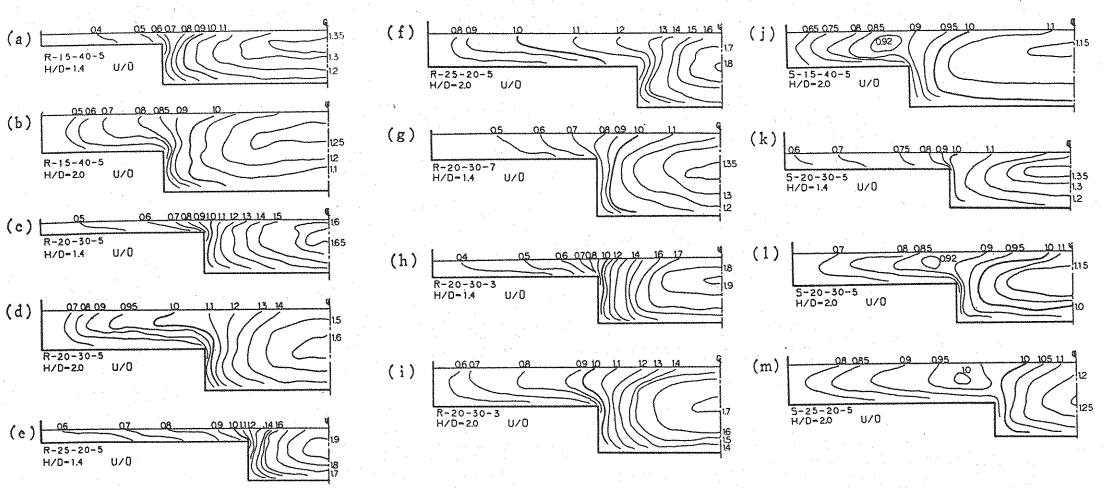

Fig . 4 Iso-velocity contours in compound channel section

that the flow structure, comprising the deep fast moving flow in the compound channel and the shallow slow moving one in the floodplain, is no longer a two dimensional free shear flow parallel to the bottom.

(B) Effects of floodplain roughness

(1) The high velocity-region mentioned above cannot be observed in the compound channel of Type-R, even if H/D is large.

(2) The density of iso-velocity contours for Type-R becomes high near the junction in the main channel as compared with those for Type-S .

(C) Effects of floodplain width and height of the main channel

(1) The influence of B_f/B on the structure of the iso-velocity contours is uncertain, regardless of Type-R and Type-S.

(2) Paying attention to the normalized mean velocity $U/\bar{U}$($\bar{U}$: cross sectional mean velocity), it is noticed that $U/\bar{U}$ in the main channel becomes small as B_f/B increases, and that $U/\bar{U}$ in the floodplain becomes large conversely. This tendency can be easily extracted in Type-R.

(3) From the iso-velocity contours of flows in the compound channel with same B_f/B and B_m/B, it is noticed that there are few changes in them when H/D is same, regardless of the size of D. The value of $U/\bar{U}$ in the main channel, however, is seen to increase with the decrease in D.

Characteristics of Transverse Profiles of Velocity, U

Figure 5 shows the transverse profiles of velocity, U(y) at different heights, z.

(A) Effects of relative water depth

Effects of H/D are apt to be observed in the flow for Type-S. For example, U_f monotonously increases with y and has a maximum at the edge of the floodplain, when H/D is small. However, when H/D is large, the maximum velocity of U_f occurs slightly away from the edge of the floodplain , because of the high speed fluid over the floodplain.

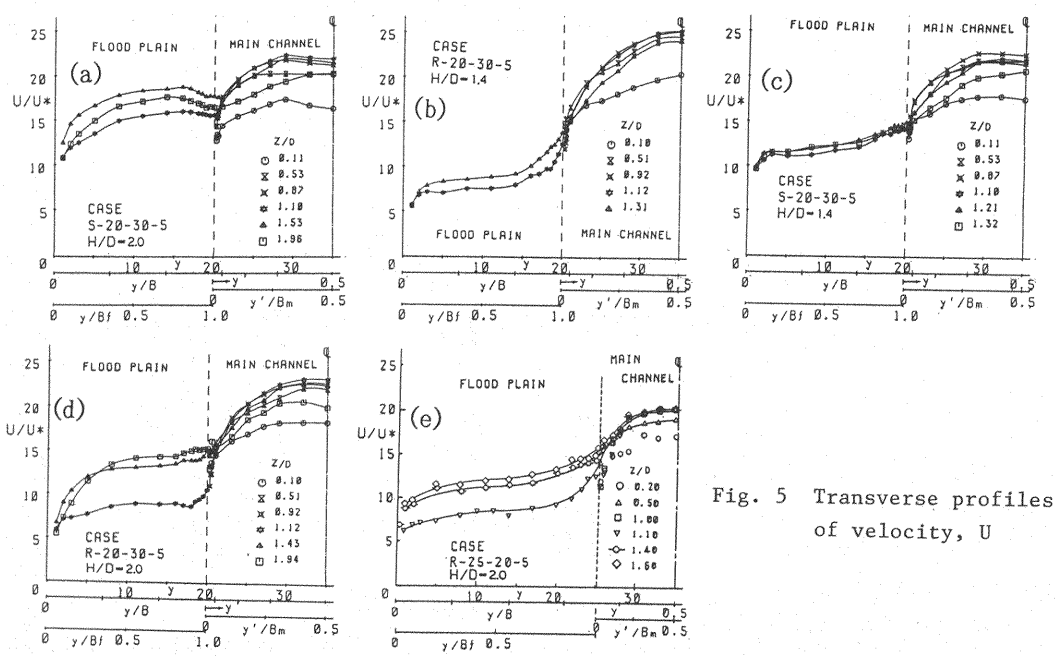

Fig. 5 Transverse profiles of velocity, U

(B) Effects of floodplain roughness

The velocity gradient, dU/dy, at the edge of the floodplain for Type-R is larger than that for Type-S under the same geometry size and H/D. It may be reasonable to interpret that the retardation of floodplain flow due to the floodplain roughness causes an increase in velocity difference between the floodplain and the main channel.

Characteristics of Vertical Profiles of Velocity, U

H/D and floodplain roughness may be considered as the main factors, which control the iso-velocity contours and transverse profiles of U. Therefore, the effects of these two factors on the vertical profile, U(z), are described in this part.

(A) Effects of relative water depth

A local retardation of U is observed near the edge of the floodplain in the main channel(near small y') in Fig.6.

(1) This phenomenon, however, becomes almost imperceptible away from the edge of the floodplain towards the center of the main channel and finally disappears at $y'=L_y$.

(2) On the floodplains, the maximum velocity occurs below the water surface when H/D is large, but it appears near the water surface when H/D is small.

(B) Effects of floodplain roughness

(1) The local retardation of U remarkably appears in the flow of Type-R rather than in Type-S. Figure 7 demonstrates the relationship between H/D and L_y. In Fig.7, L_y is normalized by the water depth in the floodplain, H_f. The plots in the graph are somewhat scattered, but L_y/H_f is within a range of 0.2-0.3 for Type-S and 0.4-0.6 for Type-R, regardless of $B_f/B(B_m/B)$ and H/D. L_y seems to depend on H_f and n_f/n_m. From this, it can be hypothysized that the interaction between the main channel and floodplain flow is strengthened by the floodplain roughness as indicated by Kawahara and Tamai(11), and relatively enlarges its spatial extent in the case of Type-R .

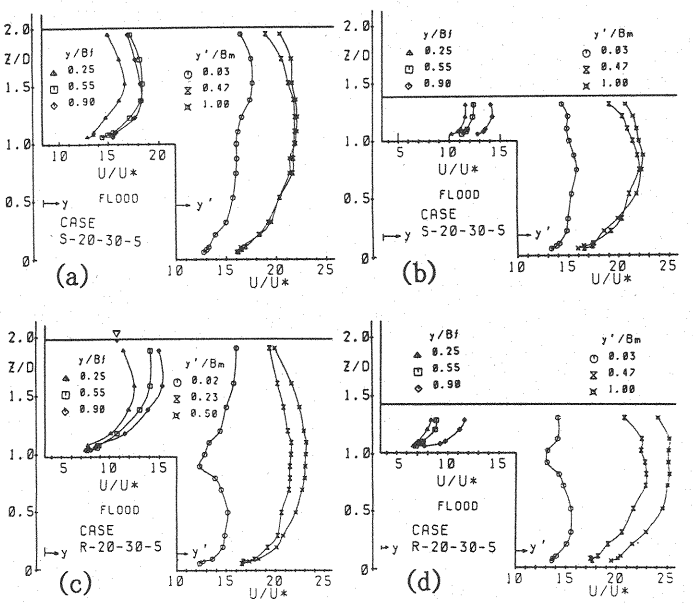

Fig. 6 Vertical profiles of velocity, U

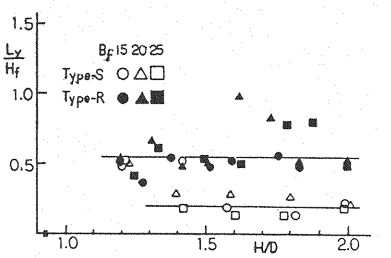

Fig. 7 Transverse scale of local retardation observed in vertical profile of velocity, U

(2) The velocity gradient, dU/dz, near the bottom on the floodplain generally becomes large with y, that is, towards the edge of the floodplain. The value of dU/dz is larger for Type-R than Type-S as well as dU/dy.

RESULTS AND DISCUSSIONS OF TURBULENCE INTENSITY

Characteristics of Iso-Turbulence Intensity Contours

Figure 8 shows the iso-turbulence intensity contours. It is found that high turbulence energy is produced by the interaction between the main channel and floodplain flow near the edge of the floodplain, and develops into a tongue shape.

(A) Effects of relative water depth

(1) An upward extent of the high turbulence intensity generated near the edge of the floodplain has an angle of inclination to the y-axis. This inclination decreases as H/D becomes small and a downward extent of u' can be recognized in CASE R 25-20-5(H/D=1.3).

(2) The area, which the fluid body with the high turbulence intensity occupies in the flooodplain, is also suppressed with the decrease in H/D.

(B) Effects of floodplain roughness

(1) The value of the normalized turbulence intensity, u'/u_*,(u_*: the friction velocity over the total wetted perimeter) near the edge of the floodplain for Type-R is larger than that for Type-S.

(2) Comparing u'/u_* near the edge of the floodplain with one near to the bottom in the main channel, the former is a little larger than the latter or both are equal in the case of Type-S.

(3) As far as Type-R, however, the former is larger than the latter, even with same geometry size and H/D, because of the floodplain roughness.

(C) Effects of floodplain width and height of the main channel

(1) The iso-turbulence intensity lines in the floodplain are arranged almost parallel to the bottom for a large B_f/B such as CASE S-25-30-5. They, however, construct a vertical arrangement as shown in Fig.8(c) when B_f/B is small, regardless of H/D. This implies that the contribution of side wall turbulence to U(y) in the floodplain gets smaller with the decrease in B_f/B and is independent of H/D.

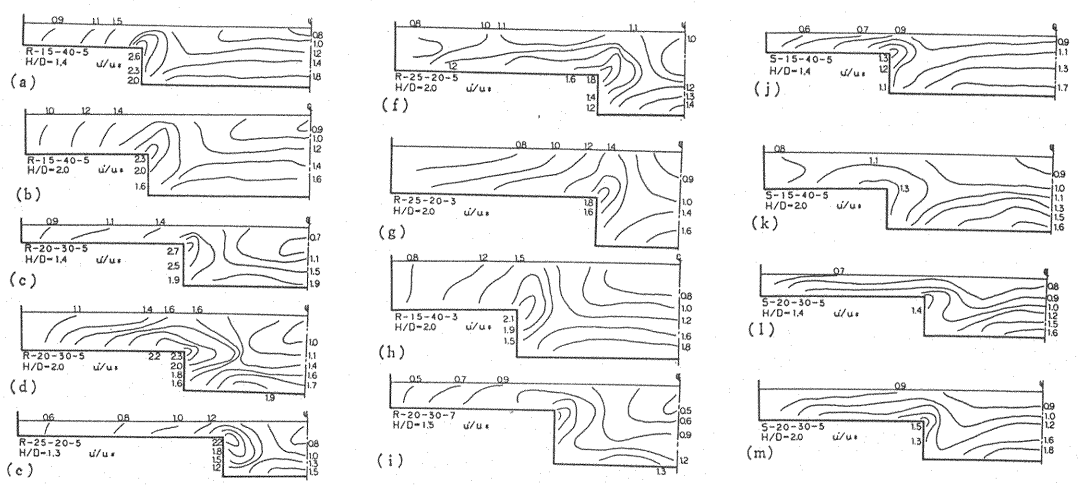

Fig. 8 Iso-turbulence intensity contours in compound channel section

(2) In the main channel, the iso-turbulence intensity contours are parallel to the bottom as B_f/B is large. From this result, it is known that the wall turbulence, produced near the bottom, has a strong effect on the whole structure of turbulence in the main channel as B_m/B becomes large.

(3) It seems that the influence of D on the contours of u' in the compound cross section is very small.

Characteristics of Transverse Distribution of u'

Figure 9 demonstrates the transverse distributions of the turbulence intensity, u'(y) at different z. It is noticed that u' at z/D=0.2 basically increases away from the side wall of the main channel towards the center of the compound channel . For z/D>1, u' has a maximum at the edge of the floodplain and decreases towards the center of the main channel. In the floodplain, an increase in u' with y appears more clearly near the bottom than near the water surface.

(A) Effects of relative water depth

(1) In the floodplain, u'/u_* near the bottom at the edge of the floodplain decreases as H/D becomes large. This is essentially identical with the decrease in dU/dy at the edge of the floodplain with the increase in H/D .

(2) The value of u'/u_* at z/D=1.0 has its maximum at the edge of the floodplain, and decreases towards not only the side wall in the floodplain but also the center in the main channel. When H/D is small, especially, an absolute value of du'/dy is largest at the edge of the floodplain for any height of z/D>1(See Fig.9(a)).

(B) Effects of floodplain roughness

The value of u'/u_* for Type-R is generally 1.5-1.7 times larger as one for Type-S in the floodplain. To be precise, the increase-rate of u'/u_* is largest at the edge of the floodplain and decreases towards the side of the wall. On the other hand, an increase in u'/u_* due to the floodplain roughness is observed near the bottom in the floodplain, but becomes insignificant towards the water surface.

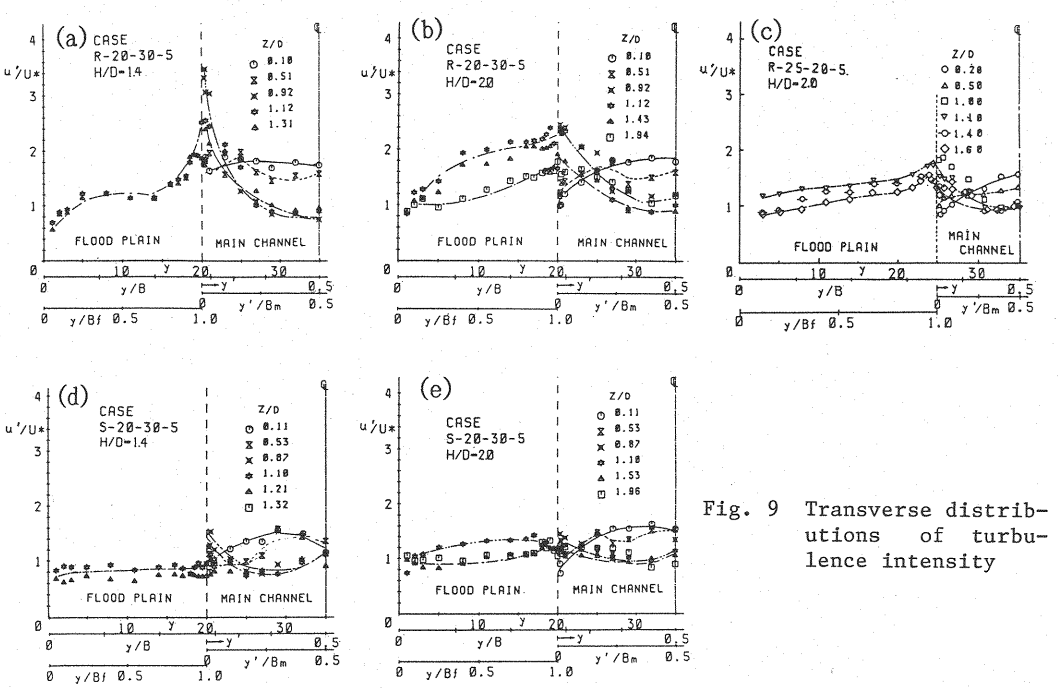

Fig. 9 Transverse distributions of turbulence intensity

(C) Effects of floodplain width and height of the main channel

From Figs.8 and 9, it is noticed that u'/u_* at the edge of the floodplain decreases with the increase in B_f/B under the same channel size and H/D. No large difference, however, is observed in the shape of u'(y).

Characteristics of Vertical Distribution of u'

Figure 10 shows the vertical distributions, u'(z), at different transverse positions, y and y'. The fundamental characteristics of u'(z) in the main channel will be described below.

(1) Near the side wall , u'(z) has its maximum value at z=D and decreases upward towards the water surface and downward towards the bottom. There exists a negative correlation between U(z) and u'(z) near the edge of the floodplain as shown in Fig.11. From this fact, it can be estimated that a fluid body with high turbulence intensity due to the interaction near the main channel /floodplain junction will enter into the main channel flow, which has a relatively high velocity.

(2) Comparing the negative correlation between u'(z) and U(z) in Type-R with that in Type-S, the former is higher than the latter, because the interaction between the main channel and floodplain flow for Type-R is stronger than that for Type-S.

(3) At the center, the maximum u', u'_{max}, occurs near the bottom and u' decreases towards the water surface, but there are also some experimental cases that u' rises near the water surface again. In the floodplain, u' basically decreases away from the bottom towards the water surface, but this decrease in u' gets clearer in the section near the edge of the floodplain.

As shown in Fig.12, however, u'(z) at the center in the main channel is different from the exponential profile reflected by the wall turbulence in rectangular open channels, which is expressed as $u'/U=A_S\exp(-B_S z/D)$. A_S and B_S are constants. All data belong to the experimental case of $B_m/B=0.43$ and H/D=1.7-2.0, regardless of the value of D. Especially, a deviation of the plots from the exponential curve becomes large for z/D>1.0-1.5, and is larger in Type-R than in

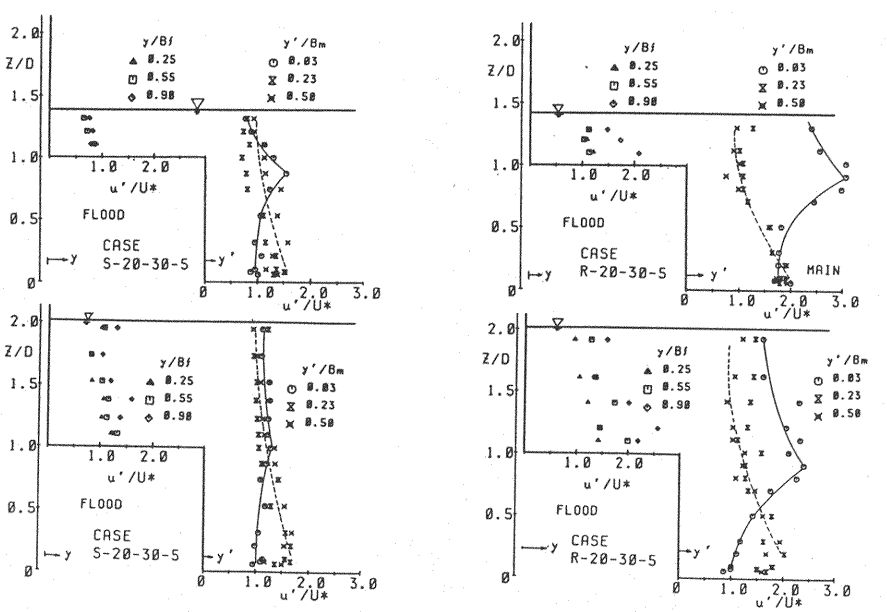

Fig. 10 Vertical distributions of turbulence intensity

Type-S. On the other hand, near the side wall in the main channel, u' seems to decrease exponentially from the floodplain height towards the bottom as shown in Fig.13. The two curves in Fig.13 express exponential distributions and are adapted for flows in the compound channel section with B_m=0.3m, B_f=0.2m and D=0.05m. The difference between two curves and experimental data appears for z/D<0.3-0.5. From these results, it is suspected that the interaction may have an effect on the turbulence at the center of the main channel but the wall turbulence still dominates the turbulence structure near the corner in the main channel.

Next, the effects of H/D, floodplain roughness, B_f and D on u'(z) are discussed. The decrease in u' from z=D downward towards z=0 or upward towards z=H is clearer for Type-R than Type-S at small y'/B_m. This means that the interaction and turbulence mixing between the main channel flow and floodplain flow near z=D diminishes remarkably away from the edge of the floodplain . We were unable to find an evident variation of u'(z) by the change of H/D, B_f and D in the present experiments.

Based on the facts described above, the turbulence structure in the main channel may be proposed as the schematic view shown in Fig.14. The model explains that the turbulence, produced by the interaction, develops in region (I) and the

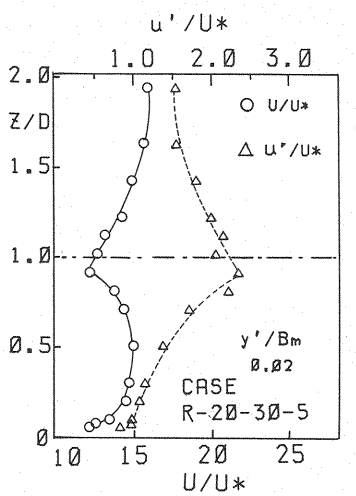

Fig. 11 Comparison of velocity with turbulence intensity profile

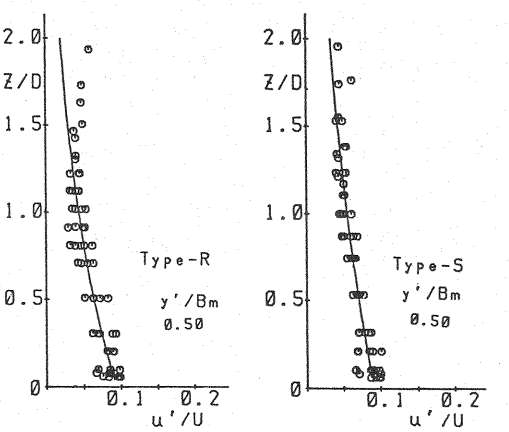

Fig. 12 Typical vertical profiles of turbulence intensity at center in the main channel

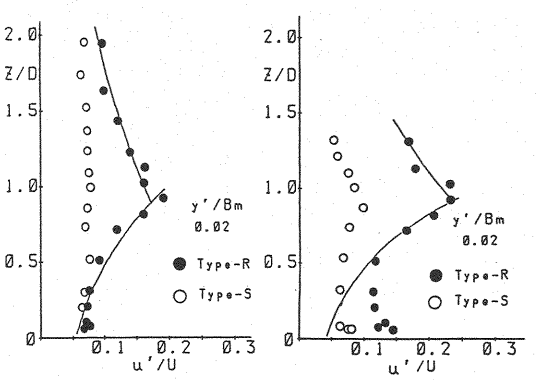

Fig. 13 Typical vertical profiles of turbulence intensity near side wall in the main channel

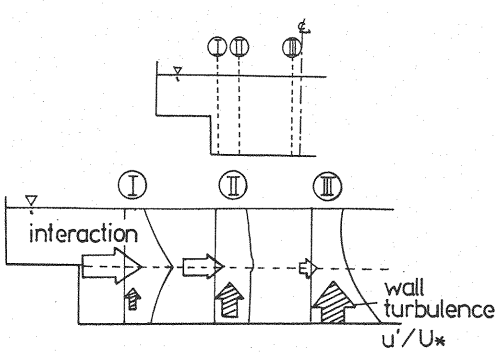

Fig. 14 Schematic view of turbulence structure

wall turbulence contributes dominantly to u'(z) in region (Ⅲ), and these two kinds of turbulence keep the balance in region (Ⅱ).

RESULTS AND DISCUSSIONS OF WALL SHEAR STRESS

Characteristics of Distribution of Wall Shear Stress

Figure 15 shows a series of wall shear stress distributions. Two kinds of τ_w distributions are presented to comprehend directly the effects of the floodplain roughness on them. τ_w is normalized by $\overline{\tau}_w$, which denotes the mean value of $\overline{\tau}_w$ over the whole wetted perimeter.

(A) Effects of relative water depth

(1) When H/D is small, τ_w in the floodplain remarkably increases near the edge of the floodplain, comparing Fig.15(a) with Fig.15(b). When H/D is large, however, τ_w remarkably increases near the side wall in the floodplain and then eventually increases towards the edge of the floodplain.

(2) Paying attention to the τ_w distribution on the side wall in the main channel, it is noticed that the maximum τ_w occurs near z=D/2 when H/D is small, but it shifts near z=D when H/D is large.

(3) The value of $\tau_w/\overline{\tau}_w$ on the floodplain increases with H/D.

(4) When H/D is large, the maximum τ_w on the floodplain occurs slightly away from the edge of the floodplain, where is located the high velocity region. From this, it is easy to see that there exists an strong correlation between the wall shear stress distribution and the mean velocity-structure.

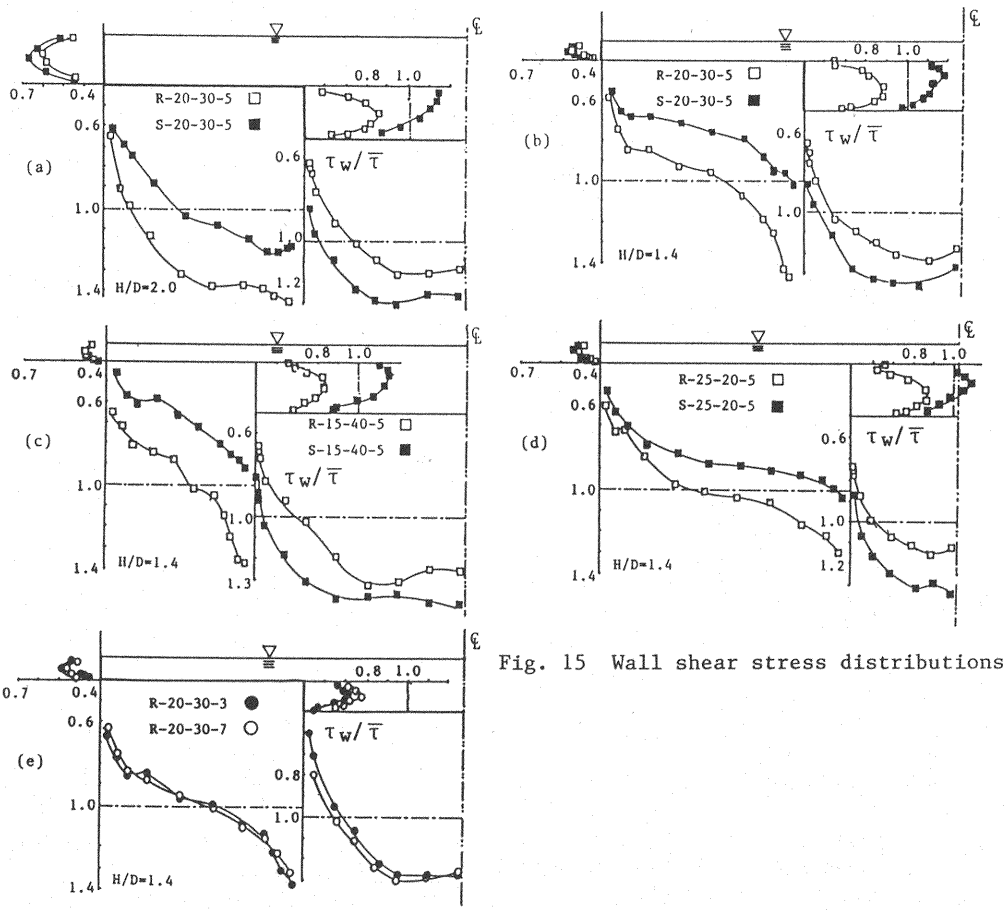

Fig. 15 Wall shear stress distributions

(B) Effects of floodplain roughness

(1) Of course , $\tau_w/\bar{\tau}_w$ for Type-R is larger than that for type-S in the floodplain, but this property is obviously opposite in the main channel, that is, $\tau_w/\bar{\tau}_w$ for Type-R is smaller than that for Type-S.

(2) The maximum τ_w in the floodplain occurs slightly away from the edge of the floodplain for Type-S, but does not appear there when H/D is large, as far as Type-R is concerned.

(3) $\tau_w/\bar{\tau}_w$ on the side wall in the floodplain and main channel are relatively larger for Type-S than for Type-R, especially when H/D is large.

(C) Effects of floodplain width and height of main channel

(1) As B_f/B increases, the increase in τ_w with y in the floodplain becomes gradual and τ_w is almost uniform at the middle part of the floodplain.

(2) On the other hand, $d\tau_w/dy$ on the bottom in the main channel becomes large away from the side wall towards the center as B_m/B decreases.

(3) It seems that τ_w profiles are almost independent of D within the present experimental conditions.

Characteristics of Apparent Shear Force

Figure 16 presents the relationships between H/D and the percentage of shear force in the floodplains and in the main channel to the total shear force, S_f/S_{all} and S_m/S_{all}, respectively. The percentage cross section of the floodplains and main channel, A_f/A and A_m/A are also shown in Fig.16. (A_f: cross section of floodplain , A_m: cross section of main channel, A: overall cross section.)

From the momentum balance equation for the main channel flow, the value of A_m/A minus S_m/S_{all} implies the apparent shear force, A_{SF}, acting on imaginary vertical interface plane between the main channel and floodplain. Based on Fig.16, it is admitted that A_{SF} enforces the main channel flow first and the floodplain flow slow. Figure 17 illustrates the relationship between A_{SF}/S_{all} and H/D with the change of $B_m/B(B_f/B)$. A_{SF} for Type-R is larger than that for Type-S under the same B_m/B and H/D. A_{SF}/S_{all} remarkably increases with H/D for H/D<1.3-1.4 and then becomes almost constant up to H/D=2.0. This tendency is similar to the result(Fig.7), obtained by Asano et al.(2), in the range of H/D≦2.0. Furthermore, A_{SF}/S_{all} increases with the decrease in B_m/B for the same H/D.

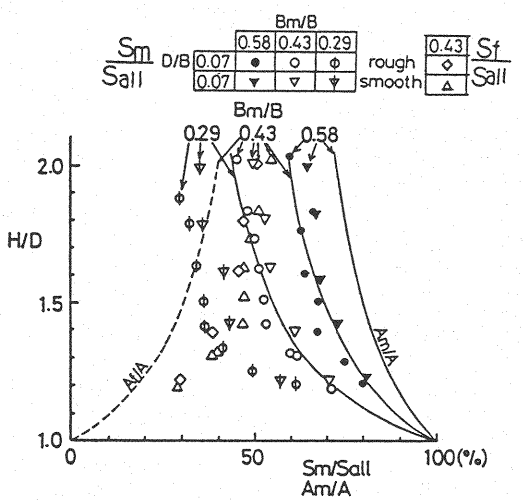

Fig. 16 Relationships between H/D and percentage of shear force in the floodplains and in the main channel

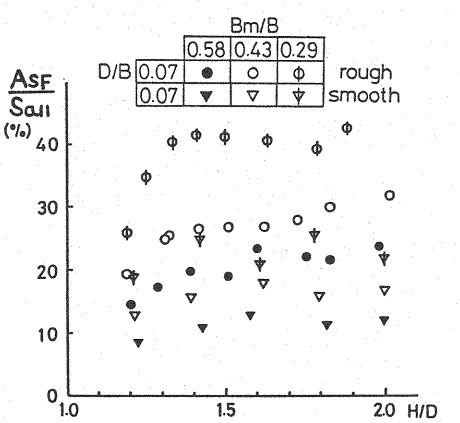

Fig. 17 Relationships between A_{SF}/S_{all} and H/D with the change of Bm/B

According to these results, if the discharge is calculated by the commonly used method, i.e. the separated channel method using the vertical interface, the overall discharge calculated by this method will become inacculate with H/D as indicated by Murota et al.(13).

CONCLUSION

The mean velocity, turbulence intensity and wall shear stress were measured and the effects of the relative height, floodplain roughness, width of the floodplain and main channel, and height of floodplain were discussed in the present study. Main conclusions are as follows:

1. The relative height and floodplain roughness among the four parameters mentioned above especially have a strong effect on the flow structures such as the mean velocity, turbulence intensity and wall shear stress profiles.

2. There exist cross correlations among the mean flow , turbulence structure and wall shear distribution. This can be supported by the following results:

(a) The extent of the high turbulence intensity due to the interaction near the main channel/floodplain junction has a positive correlation with the transverse extent of the local retardation observed in the vertical profile of the mean velocity in the main channel.

(b) The turbulence intensity at the junction is proportional to the transverse velocity gradient there, and this property is easily admitted by the comparison between Type-R and Type-S.

(c) The location, where the maximum τ_w on the floodplain appears for Type-S, changes with H/D, and this property is attributed to the existence of the high speed region in the floodplain.

3. The interaction between the main channel and floodplain flow is stronger for Type-R than for Type-S, and is also apt to pick up in the case of Type-R.

REFERENCES

1. Alavian, V. and V.H. Chu : Turbulent exchange flow in shallow compound channel, 21th IAHR Congress, Australia, pp.447-451, 1985.
2. Asano, T., Hasimoto, H. and K. Fujita : Characteristics of variation of Manning's roughness coefficient in a compound cross section, 21th IAHR Congress, Australia, pp.30-34, 1985.
3. Bommanna, G, Krishnappan and L.Y. Lam : Turbulence modeling of flood plain, J. Hydr., ASCE, Vol.112, HY-4, pp.251-266, 1986.
4. Fukuoka, S., Asano, T., Fujita, K. and A. Asano : Characteristics of flow resistance in compound cross section, Proc. of 30th Japanese Conference on Hydraulics, pp.499-504, 1986.
5. Fukuoka, S. and K. Fujita : Prediction of flow resistance in compound channels and its application to design of river courses of flow resistance in compound cross section, Proc. of JSCE, No.411/II-12, pp.63-72, 1989.
6. Gosh, S.H. and S.B. Jena : Boundary shear distribution in open channel compound, Proc. Inst. of Civil Engineering. London, England, pp. 417-430, 1971.
7. Imamoto, T. and T. Ishigaki : Experimental study on secondary flow in compound open channel, Proc. of Hydraulic Engineering, JSCE, pp.403-408, 1990.
8. Imamoto, T., Ishigaki T. and S. Inada : On the hydraulics of an open channel flow on complex cross section, Disaster Prevention Research Institute Annuals, No.25B-2, pp.509-527, 1982.
9. Imamoto, T. and T. Kuge : On the basic characteristics of an o pen channel flow in complex cross section, Disaster Prevention Research Institute Annuals, No.17B, pp.665-679, 1974.
10. Kawahara, Y. and N. Tamai : Calculation of Three-dimensional turbulent flows in a compound open channel, Proc. of 31th Japanese Conference on Hydraulics, pp.425-430, 1987.
11. Kawahara, Y. and N. Tamai : Mechanism of lateral momentum transfer in a compound open channel, 23th IAHR Congress, Ottawa, pp.463-470,1989.
12. Knight, D.W. and J.D. Demetriou : Flood plain and main channel flow

interaction, J. Hydr., ASCE, Vol.109, HY-8, pp.1073-1092, 1983.
13.Murota, A., Fukuhara T. and M. Seta : Hydraulic characteristics of compound channel flows with floodplain roughness, Proc. of Hydraulic Engineering, JSCE, pp.409-414, 1990.
14.Pasche, E, Rouve, G. and P.Eversa : Flow in compound channels with extream flood-plain roughness, 21th IAHR Congress, Australia, pp.384-389, 1985.
15.Prions, P., Townsend, R. and S. Tavoularis : Structure of Turbulence in compound channel flows, J. Hydr., ASCE, Vol.111, HY-9, pp.1246-1261, 1985.
16.Radojkyovic, M. and Djordjevic, S. : Computation of discharge distribution in compound channel, 21th IAHR Congress, Australia, pp.368-371, 1985.
17.Rajanatnum, N. and R.M. Adhadi : Interaction between main channel and flood-plain flows, J. Hydr., ASCE, Vol.105, HY-5, pp.573-588, 1978.
18.Tominaga, A., Ezaki, K. and S. Kabatake : Three dimensional turbulent structure in compound open channel flows, Proc. of JSCE, Vol.417, II-13, pp.129-138, 1990.
19.Yen, C.L. and D.E. Overton : Shape effects on resistance in flood-plain channel, J. Hydr., ASCE, Vol.99, HY-1, pp.219-238, 1973.
20.Wormleaton, P., Allen, J. and P. Hadjipanos : Discharge assessment in compound channel flow, J. Hydr., ASCE, Vol.108, HY-9, pp.975-994, 1973.

APPENDIX - NOTATION

The following symbols are used in this paper:

- A = overall cross section;
- A_f = cross section of floodplain;
- A_m = cross section of main channel;
- A_{SF} = apparent shear force acting on imaginary vertical interface plane between the main channel and floodplain;
- B = width of compound channel;
- B_f = width of floodplain;
- B_m = width of main channel;
- D = height of the main channel;
- H = water depth in the main channel;
- H_f = water depth in the floodplain;
- H_{max}, H_{min} = maximun and minimum water depth in the main channel;
- L_y = distance from the side wall in the main channel where a local retardance in U(z) disappear;
- n_f = Manning's roughness coefficient in the floodplain;
- n_m = Manning's roughness coefficient in the main channel;
- Q = discharge;
- Q_{max}, Q_{min} = maximum and minimum discharge;
- S_{all} = overall shear force;
- S_f = shear force in the floodplain;
- S_m = shear force in the main channel;
- τ_w = wall shear stress;
- τ_w = mean wall shear stress over whole wetted perimeter;
- U = streamwise velocity;
- u' = turbulence intensity;
- $U(y)$, $U(z)$ = velocity profile of U in the direction of y and z;
- $u*$ = friction velocity over the total wetted perimeter;
- y = transverse distance from the side wall in the floodplain;
- y' = transverse distance from the side wall in the main channel;
- z = vertical distance from the bottom in the main channel.

(Received July 23, 1990; revised November 26, 1990)